



# City Research Online

## City, University of London Institutional Repository

---

**Citation:** Gowree, E.R. & Atkin, C.J. (2016). On the excitation of Tollmien-Schlichting waves due to surface vibration. Paper presented at the 52nd 3AF International Conference on Applied Aerodynamics, 27-29 Mar 2017, Lyon, France.

This is the accepted version of the paper.

This version of the publication may differ from the final published version.

---

**Permanent repository link:** <http://openaccess.city.ac.uk/17554/>

**Link to published version:**

**Copyright and reuse:** City Research Online aims to make research outputs of City, University of London available to a wider audience. Copyright and Moral Rights remain with the author(s) and/or copyright holders. URLs from City Research Online may be freely distributed and linked to.

---

City Research Online:

<http://openaccess.city.ac.uk/>

[publications@city.ac.uk](mailto:publications@city.ac.uk)

---

# ON THE EXCITATION OF TOLLMIEN-SCHLICHTING WAVES DUE TO SURFACE VIBRATION

Erwin R Gowree<sup>(1)</sup> and Chris J Atkin<sup>(2)</sup>

<sup>(1)</sup>City, University of London, EC1V 0HB, UK, [erwin.gowree.2@city.ac.uk](mailto:erwin.gowree.2@city.ac.uk)

<sup>(2)</sup>City, University of London, EC1V 0HB, UK, [chris.atkin.1@city.ac.uk](mailto:chris.atkin.1@city.ac.uk)

## ABSTRACT

The effect of localised surface vibration on the stability of a Blasius boundary layer was studied. First it was demonstrated that small amplitude vibration of the order of less than  $10\mu m$  can artificially excite Tollmien-Schlichting (TS) waves provided that the frequency of excitation was within the frequency band of the naturally occurring disturbance in the freestream environment. Longitudinally aligned motors generated more energetic TS wave and the growth rate increased with increasing number of live motors. But when a combination of both longitudinally and transversely align motors was tested a reduction in the growth rate was observed even when the total number of motors was larger than the most amplified case which was generated by 5 motors along the longitudinal axis.

## 1. INTRODUCTION

From the “roadmap” to transition presented by Saric et al. [7] which was inspired by previous study of Morkovin et al. [5], the receptivity process is identified at the “heart” of the transition process. During the receptivity process environmental disturbances in the freestream which exist in the forms vortical and acoustic perturbations penetrate the boundary layer and excite instability waves while interacting with surface non-uniformities and inhomogeneities and also leading edge curvature. Once excited through the receptivity process instability waves grow accordingly with linear stability theory in very low turbulence environment. The effect on surface non-uniformities and leading edge have been intensively reviewed by Saric et al. [7] with an assessment of the progress made both experimentally and numerically, but the effect of vibration was only limited to leading edge oscillations. In the early 1980’s, the problem of surface or wall vibration attracted a lot of interest in Novosibirsk and theoretical studies by Terent’ev [8] demonstrated that harmonic oscillations of a plate could potentially excite instability waves in the form of TS waves which grows

accordingly with linear stability theory. Further experimental evidence was provided by Gilev [1] who also showed that transition due to TS instability could be delayed by damping the artificially excited TS wave by a phase-shifted excitation of the vibrating surface. This behaviour was also observed during the experiment of Kim et al. [2] but the similarity of this control technique with the Kramer-type compliant surfaces, in reference [3] and [4] is yet to be determined. From a detailed study of Ruban et al. [6], some light was shed into the physical mechanism through which TS waves are excited from surface vibration. They postulated that a Stokes layer is generated due to pressure perturbation outside the boundary layer, the Stokes layer is unable to produce any TS wave on its own as the characteristic wavelength of perturbation field is significantly larger than that of a TS wave. The main mechanism for the wavelength conversion is through interaction with localised wall roughness over a certain streamwise region.

Due to renewed interest in laminar flow aircraft this problem was revisited in the context of natural laminar flow control. Therefore, the current investigation was aimed at understanding the effect of localised small amplitude vibrations on an oncoming Blasius boundary layer and to confirm whether they can excite Tollmien-Schlichting type instability waves which would amplify and breakdown to turbulence. First a frequency analysis was conducted to identify the critical modes and secondly the amplitude of vibration was varied by changing the number of live vibrating motors over the vibrating panel. Further testing was conducted where a combination both longitudinally and transversely orientated motors were excited.

## 2. EXPERIMENT

The experiment was conducted in the low turbulence wind tunnel at the Gaster Laboratory at City, University of London. The tunnel has a return circuit with a test section of  $0.91m \times 0.91m \times 4m$ , where a turbulence in-

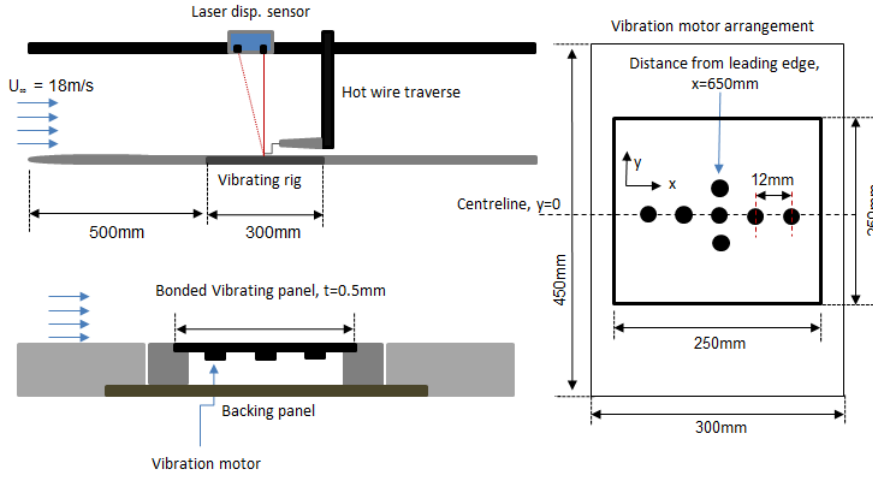


Figure 1: Schematic illustration of the top view (right) and side view (left) of the experimental model and the vibration rig set-up

tensity level,  $T_u$ , less than 0.01% can be achieved with a flat plate model inside, for a freestream velocity ranging from  $10m/s$  to  $40m/s$  and frequency bandpass set within the range of  $2Hz$  to  $2kHz$ . Hot wire measurements were made along a  $0.91m \times 2.0m$  aluminium flat plate mounted vertically between the ceiling and the floor of the tunnel. The leading edge of the flat plate was a half ellipse and also equipped with a trailing edge flap and a trim tab to adjust the location of the stagnation point and to ensure a close to zero pressure gradient condition over the majority of the plate. This was confirmed by 13 local static pressure measurements using surface mounted pressure taps. The flat plate had a rectangular cut through starting at  $0.5m$  from the leading edge and extending to  $0.8m$ , to house the vibration rig represented schematically in figure 1. A  $0.5mm$  deep recess was machined out of the  $300mm \times 450mm$  insert panel to house a  $250mm \times 250mm \times 0.5mm$  flexible Aluminium sheet which was excited by  $12mm$  diameter Precision Micro-drives coin style vibration motors mounted underneath the sheet. The vibration motors were driven by a sinusoidal voltage signal generated from NI Labview and amplified by an audio amplifier to provide the required amount of current. A series of different configurations were tested, where the motors were aligned along a single axis either along the longitudinal or the transverse axis or a combination of both. The motors were driven for a frequency range of  $60Hz \leq f \leq 172Hz$  as a parametric analysis to identify the most dominant mode and the amplitude of the vibration was controlled by varying the number of live motors after having chosen a desired input voltage to the motors.

The motors were designed in such a way that the axis of spin was normal to the flat face which was bonded under the membrane and therefore the primary oscillation was tangential to the wall. Due to the rigidly supported ends this also produced a normal deflection of the membrane in the normal direction but significantly smaller than if the axis of spin was parallel to the membrane's surface. This was beneficial in ensuring that the

deflection of the membrane was of the order of microns and hence would not introduce significant amplification of the instability wave purely due to surface deformation. The mean and fluctuating velocity components over the vibrating sheet were captured using hot wire anemometry, where the probe could be positioned at a desired wall reference position determined by the Micro-Epsilon laser displacement sensor which had a resolution of  $\pm 7\mu m$  and a frequency response of  $1kHz$ . A National Instruments PXI system was used for simultaneous data acquisition of hot wire signal, pressure and temperature and control of a three axis traverse, excitation of the vibration motors and the wind tunnel speed which was obtained from a differential pressure transducer connected to a Pitot-static tube. The experiment was conducted at a freestream Reynolds number of  $1.2 \times 10^6$  and the hot wire signal was bandpass filtered at  $10Hz - 4kHz$  through a Krohnkite filter.

### 3. ANALYSIS OF RESULTS

#### 3.1 Unexcited case

First the unexcited Blasius flow was captured so as to analyse the unperturbed base-flow. The hot wire signal was converted into the streamwise mean,  $U$  and fluctuating,  $u'$  velocity components by applying King's law obtained from a calibration. Using Matlab the fluctuating velocity component within the boundary layer could be expressed in the frequency domain using an FFT algorithm, as shown by the spectral plot at the top of figure 2. A dominant low frequency peak is observed at approximately  $29Hz$  followed by a harmonic at approximately  $58Hz$  at both streamwise positions, which was related to the vibration of the main flat plate. This was confirmed by the spectra of the signal from the laser displacement shown at the bottom of figure 2. Unfortunately, this signal was slightly more vulnerable to background noise especially mains which was represented by the peak at  $50Hz$  and the odd harmonics. The higher frequency noise was an artefact of the higher sampling rate during the data

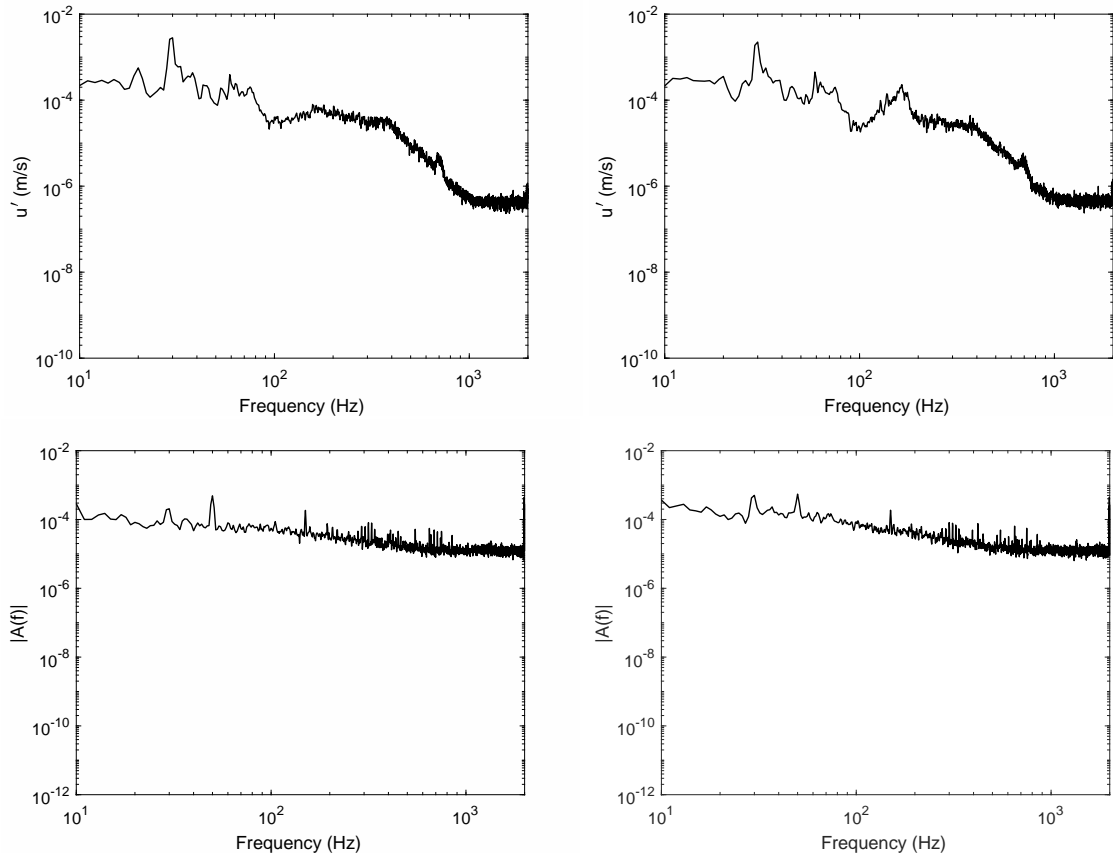


Figure 2: FFT of the hot wire signal at the top and the laser displacement sensor at the bottom for the unexcited Blasius flow at  $x = 1000mm$  and  $x = 1200mm$ , left and right respectively. The hot wire measurements were at  $y \approx 1.5mm$ .

acquisition which was four times higher than the maximum frequency response of the sensor. From the hot wire spectra, mainly at  $x = 1200mm$ , where the intensity was higher a rise in intensity was observed within the frequency bandwidth of  $100 - 200Hz$  and this was related to the natural occurring instability waves within the absence of artificially excited disturbances.

### 3.2 Selection of excitation frequency

First a frequency analysis was conducted to identify the dominant frequency while driving 5 motors aligned along the longitudinal axis and was expected to sufficiently excite the instability waves. The spectra of the corresponding excitation frequencies are shown in figure ???. Once again the low frequency peak due to the main plate vibration was present in all four cases. For the lowest excitation frequency of  $60Hz$ , no distinctive peak was observed in the spectra, however it has to be noted that this frequency was very close to the  $1^{st}$  harmonic of the main plate vibration frequency. Upon doubling this forcing frequency, a sharp peak is observed in the bottom left of figure ??? corresponding to  $120Hz$  mode which could potentially develop into an instability wave. At the highest excitation frequency of  $172Hz$  a sharper peak was observed and this appeared to be one of the most amplified modes which was in line with previous linear stability analysis of a Blasius base flow. At this excitation frequency the

flexible vibration panel was operating past its natural frequency where the  $1^{st}$  mode was determined to be at approximately  $56Hz$  and the  $2^{nd}$  mode at  $84Hz$ . However, it was very interesting to note that at an excitation frequency of  $86Hz$ , the hot wire captured both the fundamental and the  $1^{st}$  harmonic at  $172Hz$  which was more energetic than the fundamental excitation mode. From the FFT the amplitude of the fluctuating velocity component was extracted for each corresponding forcing frequency at different positions through the boundary layer and the profiles are presented in figure 3. For the excitation frequencies of  $120Hz$  and  $172Hz$  the amplitude profiles confirmed the presence of a TS wave with an inner and outer lobe, whereas in the case of  $f = 60Hz$  and  $f = 86Hz$  it was clear that at these frequencies instability waves were damped. However, when the amplitude corresponding to the  $1^{st}$  harmonic of the  $86Hz$  forcing frequency was extracted the profile shown on the right of figure 4 confirmed the presence of a TS mode again at  $172Hz$ . From the profile shown on the left, the mode due to the 1st harmonic of the forcing at  $60Hz$  was rather weak possibly due to the lower amplitude of deflection of the vibrating plate.

The evolution of these modes could be tracked downstream by plotting the local maximum in the amplitudes at each streamwise position as shown in figure 5. In the unexcited case, due to the very low amplitudes of the fluctuations the hot wire signal had to be amplified by a gain

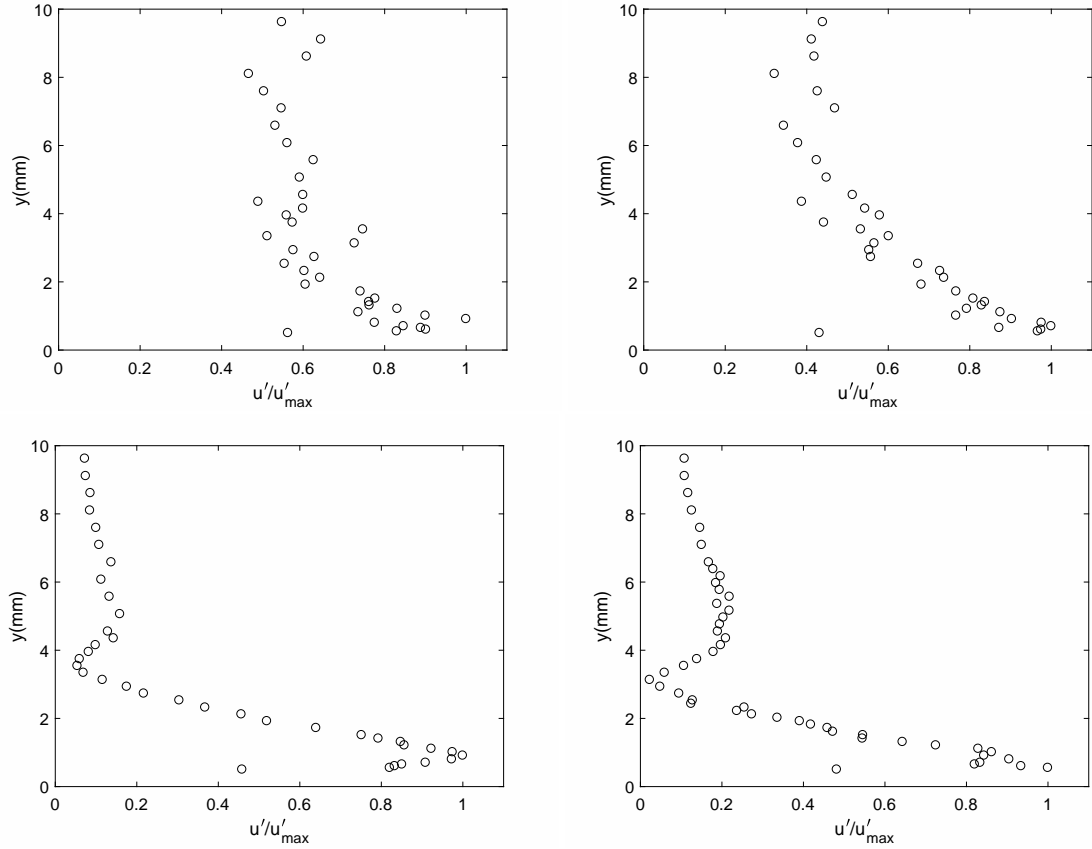


Figure 3: Fluctuating velocity component profile normalised by the maximum value, for a fundamental forcing frequency of  $f = 60Hz$ , top-left,  $f = 86Hz$ , top-right,  $f = 120Hz$ , bottom left and  $f = 172Hz$ , bottom right. The measurements were made at  $x = 120mm$  and at  $y \approx 1.5mm$ .

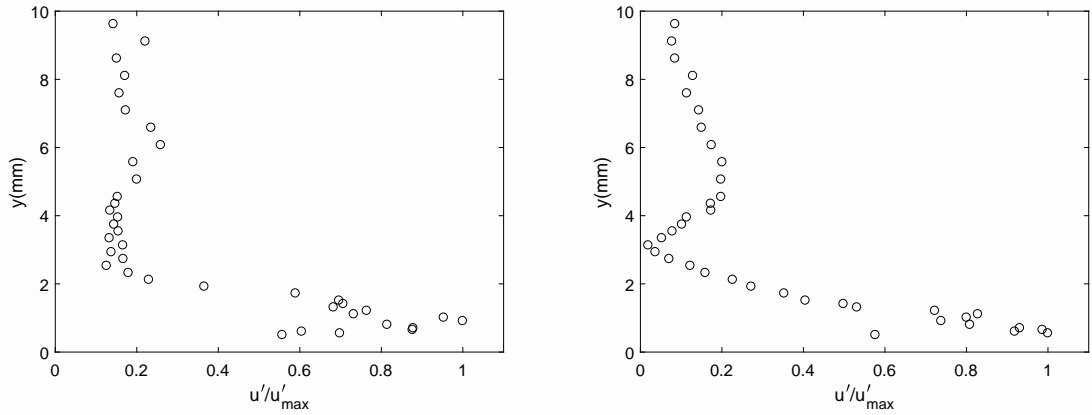


Figure 4: Fluctuating velocity component profile normalised by the maximum value, of the 1<sup>st</sup> harmonic mode of the fundamental forcing frequency of  $f = 60Hz$ , left,  $f = 86Hz$ , right. The measurements were made at  $x = 120mm$  and  $y \approx 1.5mm$ .

of  $60dB$  and this affected the signal to noise ratio, leading to a larger scatter in the data. For  $550mm \leq x \leq 750mm$ , even in the unexcited case the fluctuations were slightly higher and peaked at  $x = 650mm$ , this was due to sagging of the thin vibrating sheet when it was mounted to the main insert panel which was in turn fixed to the main flat. The maximum deflection was less than  $0.1mm$  over the whole length of the plate and from figure 5 since these

velocity fluctuations were rapidly damped downstream, at  $x > 800mm$ , this non-uniformity was therefore not sufficient to excite any instability wave. Over the vibrating panel, it was interesting to note that the near-field transients of the  $172Hz$  mode grew non-monotonically and after recovering at  $x \geq 750mm$  it started growing exponentially similar to what would be expected from linear theory. However, the growth rate of the  $120Hz$  mode was

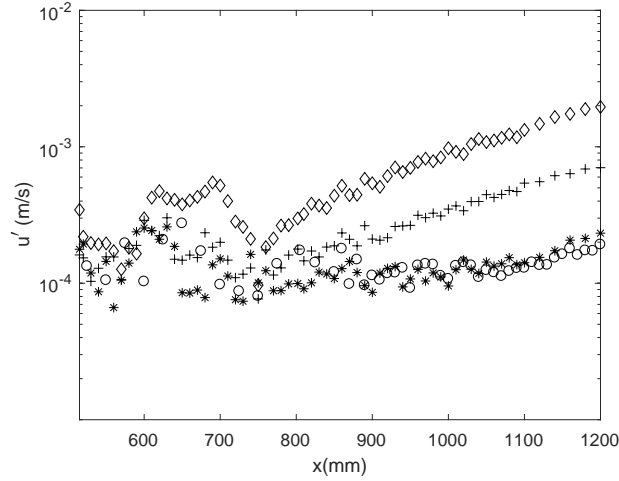


Figure 5: The amplitude of TS wave along the streamwise direction, for the unexcited case and the excited cases where the TS mode was extracted at  $f = 120\text{Hz}$ ,  $f = 172\text{Hz}$  and the first harmonic mode ( $2f$ ) of the excitation at  $f = 86\text{Hz}$ , represented by ‘o’, ‘\*’, ‘◊’ and ‘+’ and respectively.

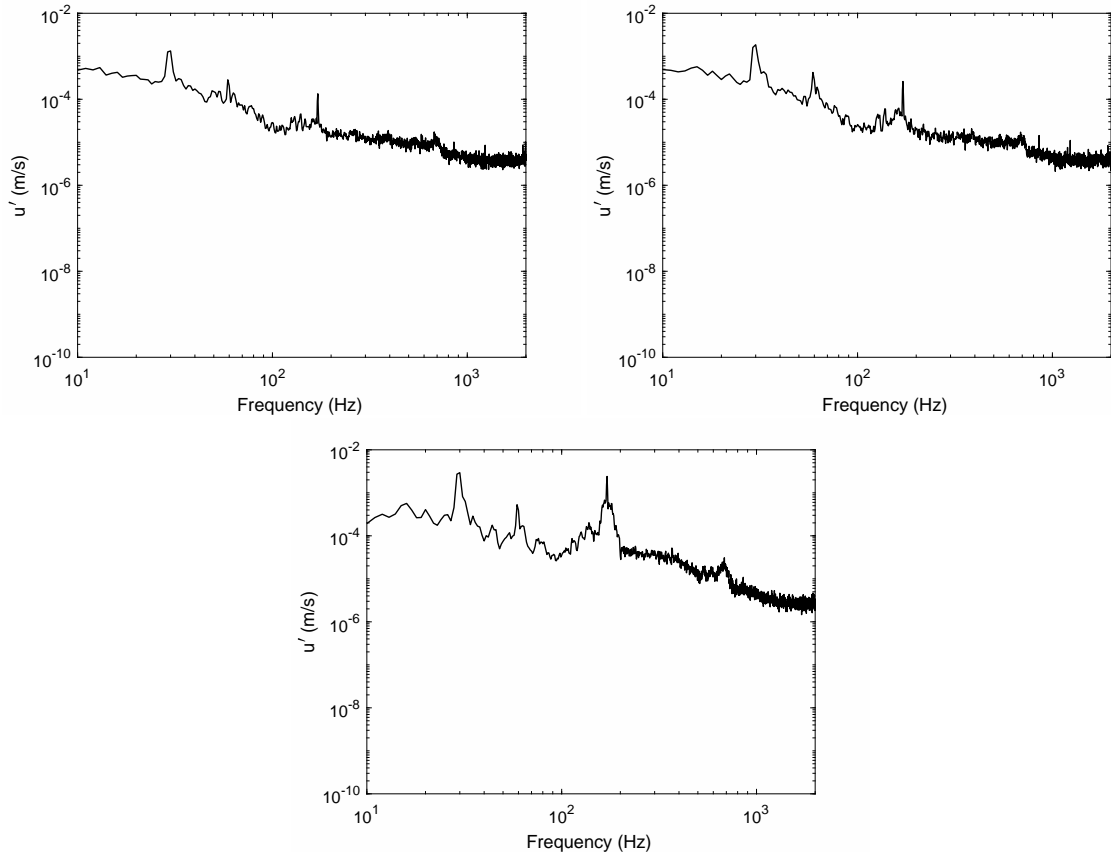


Figure 6: FFT of the fluctuating hot wire signal at a constant excitation frequency,  $f = 172\text{Hz}$ , but varying voltage input to the motors, top-left,  $V_{rms} = 2.0\text{V}$ , top-right,  $V_{rms} = 2.5\text{V}$  and bottom  $V_{rms} = 3.2\text{V}$ . The measurements were at  $x = 1200\text{mm}$  and  $y \approx 1.5\text{mm}$ .

not that significant and was almost at the same level of the unexcited case, even though the amplitude profiles showed the presence of a TS wave. However, it was interesting to note that again the 1<sup>st</sup> harmonic of the 86Hz forcing also grew similarly to the 172Hz forcing, but at a lower rate. This confirmed that the only TS mode

that could be excited was within the frequency band of the naturally present modes between 120Hz to 200Hz as shown in figure 2.

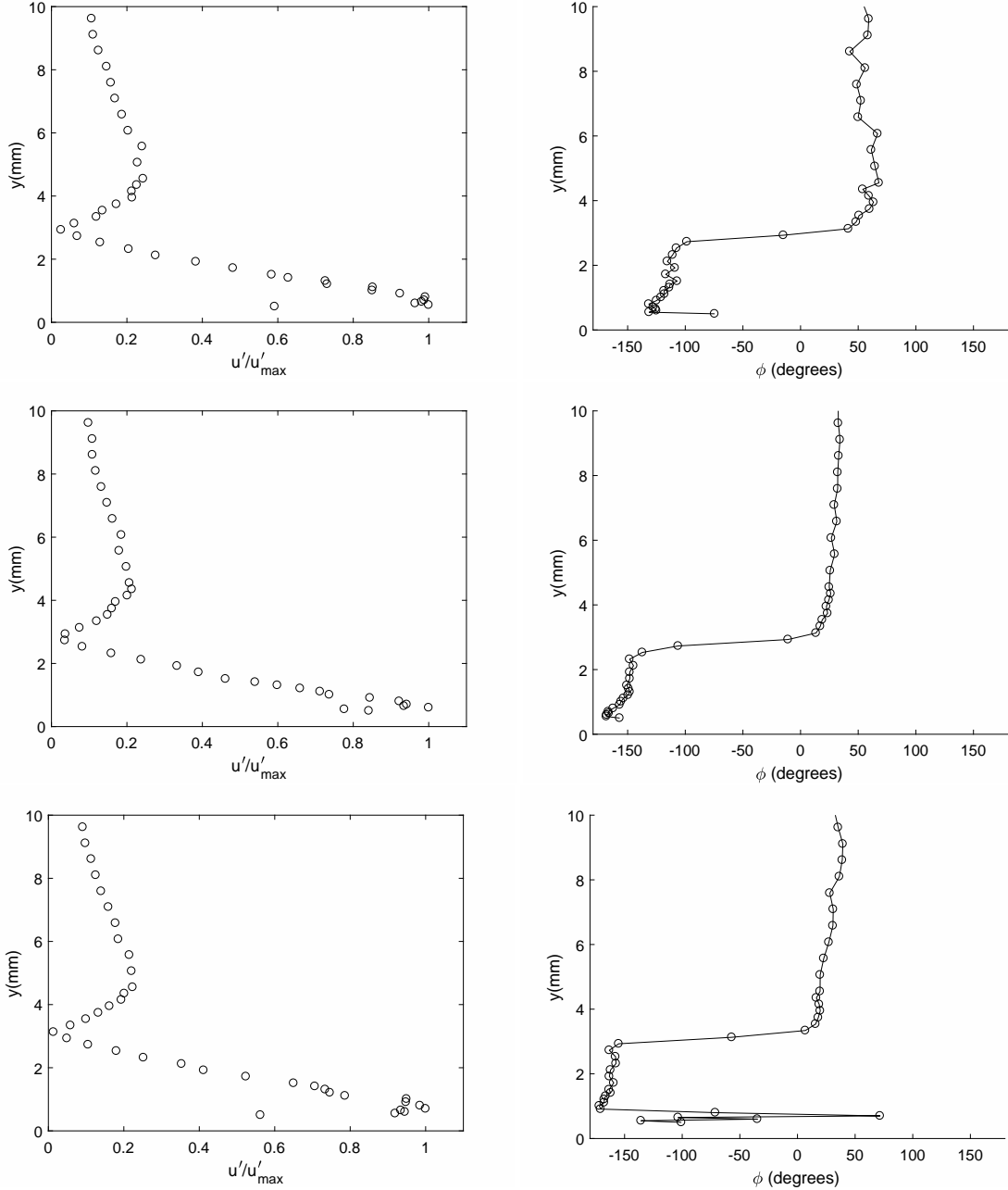


Figure 7: Fluctuating velocity component (right) and phase angle profile for a fundamental forcing frequency of  $f = 172Hz$  by 1 motor, top, 3 motors, middle, 5 motors, bottom all aligned along the longitudinal axis within the centre-plane. The measurements were at  $x = 1200mm$  and  $y \approx 1.5mm$ .

### 3.3 Effect of excitation amplitude

The results presented in section 3.2 were for five motors running simultaneously at an *rms* input voltage,  $V_{rms} = 2.5V$ , along the longitudinal axis. The amplitude of the deflection of the vibrating sheet produced by this forcing appeared to be adequate to excite the TS modes. Further increase of the input voltage should in theory increase the amplitude in the deflection and hence the excitation of more energetic TS wave which could experience non-linear growth and break down rapidly. From the spectra shown in 6, the intensity in the  $172Hz$  forcing mode increases with increasing *rms* input voltage, but even at the highest load of  $3.2V$  there was an absence of higher har-

monics or sub-harmonics which would mark the beginning of the non-linear growth stage. At  $V_{rms} = 3.2V$  the motors were driven slightly above their rated operating voltage and this would reduce their life span considerably, hence  $V_{rms} = 2.5V$  was preferred for the rest of the measurements, where each test case was conducted over a period of 12 to 15 hours. This load also appeared to generate amplitudes of the TS mode which were large enough not to be significantly affected by background noise.

Another way of varying the deflection amplitude of the vibrating sheet was by changing the number of motors ran simultaneously. Figure 8 shows when driven at  $172Hz$ ,

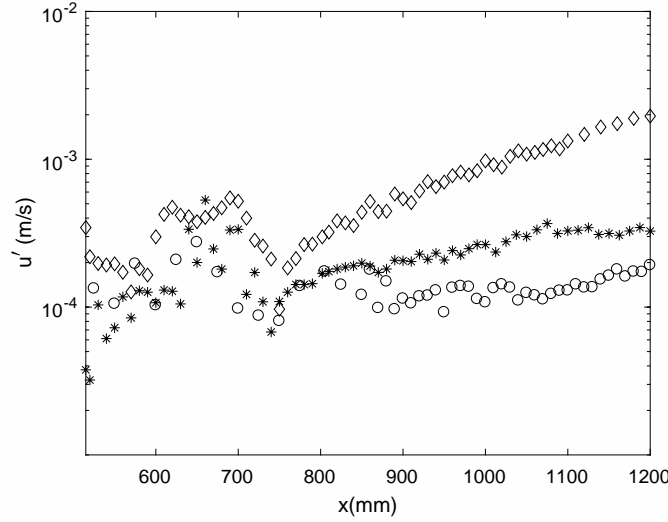


Figure 8: The amplitude of TS wave along the streamwise direction, for the unexcited case and the cases of combination of live motors excited at a frequency of  $172Hz$ . Where ‘o’ represents the unexcited case and ‘\*’ and ‘◊’ represents the case of 1 and 5 motors respectively.

even 1 motor was adequate to excite TS wave and so did 3 live motors. The growth rate of the TS wave in the streamwise direction for a single and 5 live motors can be compared in figure 8 against the unexcited case. Over right on top of the vibrating panel the trend in the near-field transients between a single motor and 5 motors are quite different. For the case of a single motor a maximum was observed at the centre of the vibrating panel and it attained similar levels to that of 5 motors. However the 5 motors case had extended region of larger amplitude peaks. The main difference in the trend of the near-field fluctuations is possibly related to the mode shape of the deflected panel which is dependent on the number of live motors and their positions. The laser displacement sensor has a resolution of  $\pm 7\mu m$ , but even with 5 live motors the sensor was not able to measure the deflection of the plate which would confirm that the deflection was definitely below  $7\mu m$ . Therefore it was difficult to capture the mode shape deflection of the plate. For the case of longitudinally align motors, once excited the mode shape of the vibrating plate does not seem to affect the growth of the TS wave beyond the recovery region at  $x \geq 800mm$  where the wave grows accordingly with linear theory.

### 3.4 Excitation along both longitudinal and transverse axis

The effect of driving the motors aligned along the transverse axis was investigated here and figure 9 confirms that forcing along this particular axis also excited TS waves. However, from figure 10, the growth rate is much lower as opposed to the 5 motors aligned in the longitudinal case as shown in figure 11. With 3 transversely orientated motors the amplitudes in the near field region was almost as low as the unexcited case. More interestingly from figure 9 the growth rate of the 3 live motor case decreases below that of the unexcited case when at  $x > 850mm$  and then

increases again at  $x > 1100mm$ . In the case of 5 motors the amplitudes dropped below that of the unexcited case also at  $x \approx 740mm$ , but increased rapidly straight after. From figure 11, the amplitude of the near field transients from both the case with the 5 motors aligned in the longitudinal and 5 motors along the transverse axis are quite similar. This suggested that the initial amplitudes of the excitation in both cases were of the same order. However, with the transverse configuration the amplitude dropped to a lower value in the recovery region at  $x \approx 740mm$ .

Due to this stabilisation effect another configuration was tested with 5 longitudinal and 3 transverse motor, which made up a total of 7 motors as the motor at the centre was accounted for in both orientation. From figure 11 higher near-field amplitude is observed in comparison to cases of the 5 motors either along the longitudinal or the transverse axis. In this case the a peak was observed at  $172Hz$  in the spectra of the laser displacement sensor and this suggested that the deflection in the vibrating sheet was larger than  $7\mu m$  and therefore the largest in comparison to the rest of the cases tested. Nevertheless, after the recovery region at  $x > 750mm$ , the growth rate was lower than the case of 5 motors along the longitudinal axis and at  $x = 1200mm$  it was even twice lower. This effect can also be observed in the subfigures on left of figure 12 and the contours on the right confirms that in both cases the initially excited instability wave was of a TS type.

## 4. CONCLUSION

It has been demonstrated that a vibrating surface can excite measurable TS instability waves even with micro displacement of the wall. From the frequency analysis it was demonstrated that the only modes that could be excited was between the frequency bandwidth of the naturally present mode which would only grow if excited artificially. From the unexcited results in the low turbu-



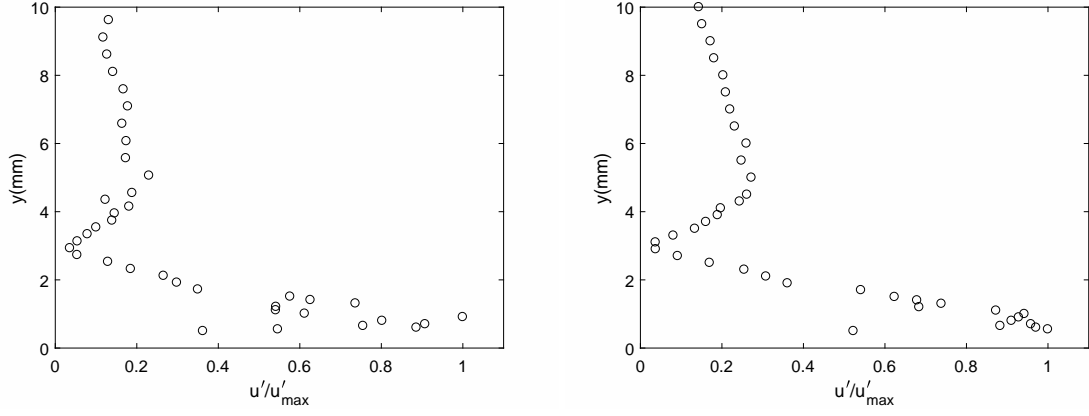


Figure 9: Fluctuating velocity component profile for a fundamental forcing frequency of  $f = 172\text{Hz}$  by 3 motor (left), and 5 motors (right) aligned along the transverse axis at  $x = 650\text{mm}$ . The measurements were  $x = 1200\text{mm}$  and at  $y \approx 1.5\text{mm}$ .

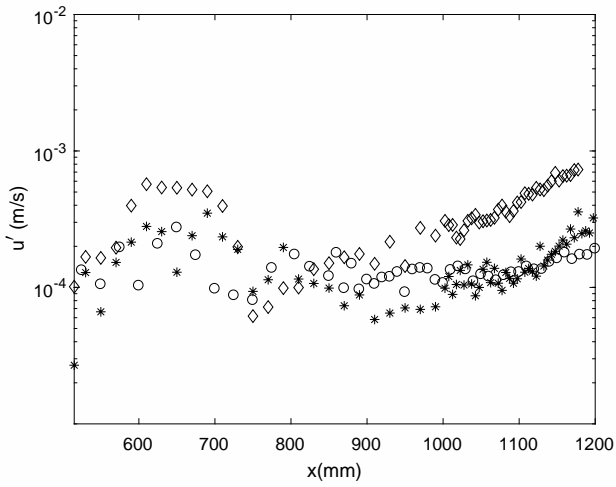


Figure 10: The amplitude of TS wave along the stream-wise direction, for the unexcited case and the excited cases where the TS mode extracted  $f = 120\text{Hz}$ ,  $f = 172\text{Hz}$  and the mode of the first harmonic ( $2f$ ) of the excitation at  $f = 86\text{Hz}$ , represented by 'o', '\*', '+ and '◇'.

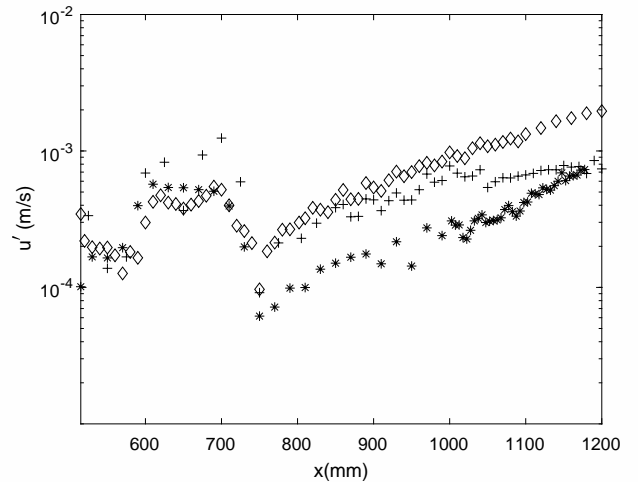


Figure 11: The amplitude of TS wave along the stream-wise direction, for the unexcited case and the excited cases where the TS mode extracted  $f = 120\text{Hz}$ ,  $f = 172\text{Hz}$  and the mode of the first harmonic ( $2f$ ) of the excitation at  $f = 86\text{Hz}$ , represented by 'o', '\*', '+ and '◇'.

lence tunnel this frequency band was between  $120\text{Hz}$  and  $200\text{Hz}$ . Thus, from the artificial forcing at  $120\text{Hz}$  and  $172\text{Hz}$ , the spectra and the fluctuating velocity and phase profiles showed clear evidence of the presence of artificially excited TS wave. At lower excitation frequency of  $60\text{Hz}$  and  $86\text{Hz}$  no TS wave was observed at the fundamental forcing frequenc. However, from the fluctuating velocity profile the  $1^{\text{st}}$  harmonic at  $120\text{Hz}$  and  $176\text{Hz}$  appeared to generate TS wave where the  $120\text{Hz}$  mode did not show much difference in growth rate with respect to the unexcited case, but the  $176\text{Hz}$  mode grew accordingly with linear stability theory. The point to be noted here is that even if the structural mode was not within the frequency band of the naturally occurring disturbance, if the harmonics of the near-field transients where within this band, they will evolve into TS modes. These modes could potentially be triggered by non-linear deformation of the

vibrating plate.

The amplitude of the plate deflection was governed by the number of live motors for a constant input  $V_{rms}$ . In most of the cases it was below  $10\mu\text{m}$  as it was not registered by the laser displacement sensor except in the case of 7 motors. Right above the vibrating panel the trend in the near-field transients was governed by the number of live motors. While aligned along the longitudinal axis an increase in the number of live motors would led to the excitation of TS wave which grew at a higher rate post the recovery region. This is potentially due to the larger amplitude of deflection and the integrated effect of larger distribution of motors. However, for the transversely orientated motors the growth rate was significantly lower and for the case of 3 motors it was even below the unexcited case within a particular streamwise region. When a combination of both longitudinal and transversely ori-

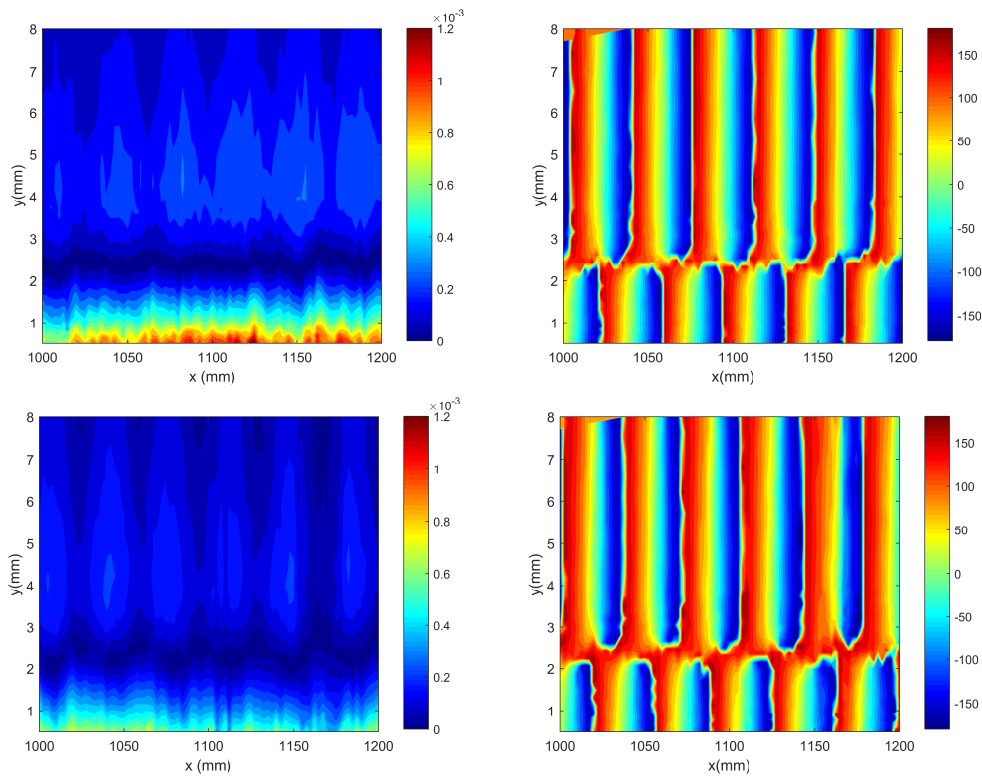


Figure 12: Fluctuating velocity component and phase angle contour for a fundamental forcing frequency of  $f = 172\text{Hz}$  by 5 motors, top, 7 motors, bottom with two transverse motors

entated motors was tested which was a total of 7 motors, even if the amplitudes of the near-field transients was larger the overall growth rate was lower than that of the case with 5 motors oriented along the longitudinal axis. Therefore, the transversely orientated motors appear to provide a small damping effect on the downstream propagating wave. At this stage it is very difficult to conclude whether the damping effect is due to structural damping or aerodynamic damping, but the present finding shows that this technique shows potential for delaying transition to turbulence from TS wave type instability. It has to be noted that all motors were ran by the same input signal therefore were supposed to be operating in-phase, unlike during the study of Gilev [1] and Kim [2]. Therefore, the current damping of the TS growth amplitude could be due to three dimensional effects generated from forcing along the transverse axis. Further investigation is encouraged to generate more insight into this technique which shows potential for delaying transition due to TS wave instability.

## ACKNOWLEDGEMENTS

The authors would like thanks the Aerospace Technology Institute for their financial support.

## REFERENCES

[1] V M Gilev. Tollmien-schlichting waves excitation on the vibrator and laminar-turbulent transition con-

trol. In V. V. Kozlov, editor, *Laminar-Turbulent Transition*, page 243. IUTAM Symposium Novosibirsk, USSR, Springer-Verlag, 1984.

- [2] S Y Kim, X Bonnardel, J P Guibergeria, and E Brocher. Transitional boundary-layer response to wall vibrations. *Smart Materials and Structures*, 3(1):6, 1994.
- [3] Max O. Kramer. Boundary layer stabilization by distributed damping. *Journal of the American Society for Naval Engineers*, 72(1):25–34, 1960.
- [4] Max O. Kramer. The dolphins' secret. *Journal of the American Society for Naval Engineers*, 73(1):103–108, 1961.
- [5] Mark Morkovin, Eli Reshotko, and Theobald Herbert. Transition in open flow systems a reassessment. *Bulletin of American Physical Society*, 39:1882, 1994.
- [6] A. I. Ruban, T. Bernots, and D. Pryce. Receptivity of the boundary layer to vibrations of the wing surface. 723:480–528, 005 2013.
- [7] William Saric, Helen Reed, and Edward J Kerschen. Boundary-layer receptivity to freestream disturbances. *Annual Review of Fluid Mechanics*, 34(1):291–319, 2002.
- [8] E.D. Terent'ev. The linear problem of a vibrator in a subsonic boundary layer. *Journal of Applied Mathematics and Mechanics*, 45(6):791 – 795, 1981.